The Impact of Coil Winding Angle on the Force of DC Solenoid Electromagnetic Actuator

Eduard PLAVEC, Ivan LADISIC, Mladen VIDOVIC

Switchgear and Controlgear Department, Koncar–Electrical Engineering Institute, Inc.,
Fallerovo setaliste 22, 10000 Zagreb, Croatia

eplavec@koncar-institut.hr, iladisic@koncar-institut.hr, mvidovic@koncar-institut.hr

DOI: 10.15598/aeee.v17i3.3338

Abstract. *This paper presents the research on the influence of coil parameter on the force of DC electromagnetic actuator. The coil parameter discussed in the paper is the angle between the windings. The research method is based on analyzing the magnetic path of DC electromagnetic actuator and on comparison of analytically obtained results with the numerical simulation results. Transient numerical simulation of DC electromagnetic actuator has been performed on the 2D axial-symmetric model using the Finite Element Method (FEM). The main contribution is the coil winding angle impact on the force of DC electromagnetic actuator. The results showed that, by reducing the coil winding angle, it is possible to increase the electromagnetic force, reduce the coil dimensions, and thus the dimensions of electromagnetic actuator.*

Keywords

Coil parameters, coil winding angle, DC Electromagnetic Actuator force, Finite Element Method.

1. Introduction

Solenoid electromagnetic actuators are electromechanical devices which convert electrical energy to mechanical energy related to linear motion [1] and [2]. They are characterized by their compact size and simple structure. Because of their reliability, simple activation and cheap production, they are widely used in many components that accompany our daily lives [3].

The DC Electromagnetic Actuators (EMA-s) usually start some kind of tripping mechanism and they need a certain force value to overcome the initial force of tripping mechanism [4]. When developing an EMA, the goal is to meet the constraints on the force and time response, while maintaining dimensions as small as possible.

The coils are the main constructional elements of an EMA. Thus, the coil parameters selection process is a prerequisite to build a fully efficient device [5]. The precise selection of coil's parameters is essential to achieve the maximum speed of the plunger. The force acting on ferromagnetic core depends on the product of current flowing through wires and number of coil turns [6] and [7].

The selection of coil parameters regarding the coil's size and number of turns is investigated in [5]. The impact of the coil diameter and length on the voltage distribution in a machine stator winding fed by PWM inverter was investigated in [8]. A study of effects on size and number of turns based on signal distribution on impedance plane diagram is performed in [9]. The influence of coil radius on electromagnetic repulsion mechanism performance is considered in [10]. However, there is no paper which investigates the impact of coil winding angle on the force of EMA, while maintaining the coil resistance constant.

In this paper, the investigation of the impact of coil winding angle on the force of DC EMA has been performed. The research method is based on analyzing the magnetic path of DC EMA and comparison with the numerical simulation results. The coil parameter discussed in the paper is the coil winding angle. The coil resistance is usually confined by the current which switch is capable of breaking. In that case, it is possible to lower the coil dimensions by coil winding procedure or by using the wire with the smaller diameter, while still maintaining the constraint on the force.

Transient numerical simulation of DC electromagnetic actuator has been performed in ANSYS Desktop Electronics software, on the 2D axial-symmetric model, using Finite Element Method (FEM). The results of

numerical simulations are compared with analytically obtained results.

2. Description and Work Principle

The basic structure of the solenoid EMA consists of a non-magnetic shaft, magnetic core, air gap, plunger, non-magnetic plate and return spring (Fig. 1). The materials of EMA's parts are stated in Tab. 1.

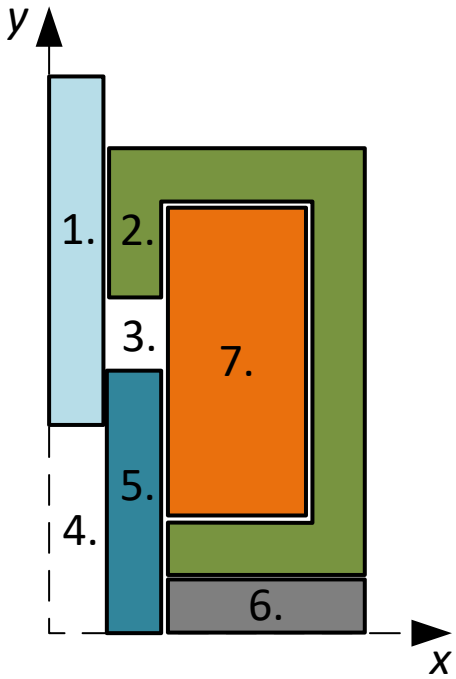

Fig. 1: The 2D axial-symmetric model of DC solenoid EMA - basic structure (cross-section).

Tab. 1: The basic parts of EMA.

Label	Part	Material
1.	Non-magnetic shaft	Stainless steel 304
2.	Magnetic core	Steel 1010
3.	Air gap	-
4.	Spring area	-
5.	Plunger	Steel 1010
6.	Non-magnetic plate	Stainless steel 304
7.	Coil	Copper

The non-magnetic shaft transfers the mechanical force of the plunger to a certain mechanism that EMA starts. Ferromagnetic core, as well as the movable ferromagnetic plunger, are the basic parts of the EMA through which the magnetic circuit closes. The core and plunger are made of electrically conductive material with non-linear B-H characteristics. The coil is wound around an insulator which is generally called bobbin. Air gap, in some references also known as the main working gap, is the place where attraction force between the plunger and the core is generated, i.e. the place of electromechanical conversion of energy. The function of return spring is to return the plunger to its initial position after switching off the EMA.

The typical response behavior of DC EMA consists of the following three operation periods [11]: sub-transient period, transient period and stopping period. In sub-transient period, there is no movement of the plunger, despite the application of excitation voltage. The magnetic flux which flows through the plunger is building the electromagnetic force acting on the plunger. When electromagnetic force overcomes the initial force of the return spring, the plunger starts to move, which is also the beginning of the transient period. The movement of plunger causes the varying magnetic flux in the EMA. Electromotive Force (EMF), which opposes to the voltage source and causes the current drop, is induced in the coil due to change of linkage magnetic flux. Stopping period starts when the plunger touches the core and finishes the movement, EMF disappears and current continues to increase.

3. Coil Winding Angle Impact - Analytical Analysis

If the solenoid EMA is observed as a magnetic circuit, it can be described using Ampere's and Hopkinson's law. If the same current flows through all windings, the Ampere's law can be written in the following form [12]:

$$\oint H\mathrm{d}l = \sum_{i}^{N} I_i = NI, \tag{1}$$

$$\oint H\mathrm{d}l = \oint \frac{B}{\mu}\mathrm{d}l = \oint \frac{\Phi}{\mu S} = NI, \tag{2}$$

where H is the magnetic field strength, I_i are the currents flowing in the N windings, B is the magnetic field, μ is the permeability of magnetic material, Φ is the magnetic flux and S is the area crossed by magnetic flux. Assuming that all the magnetic flux remains contained inside the EMA, it can be considered as a constant. Since there are two types of materials along the path of integration (magnetic material and air) and considering reluctance, $\Re = \int \frac{\mathrm{d}l}{\mu S}$, the Eq. (2) can be written as:

$$\Phi\left(\int_m \frac{\mathrm{d}l_m}{\mu S_m} + \int_a \frac{\mathrm{d}l_a}{\mu S_a}\right) = NI, \tag{3}$$

$$\Phi\left(\Re_m + \Re_a\right) = NI, \tag{4}$$

where $\Re_m$ is the magnetic material reluctance and $\Re_a$ is the air gap reluctance. The reluctances are defined as follows:

$$\Re_m = \frac{l_m}{\mu_0 \mu_r S_m}, \ \Re_a = \frac{l_a}{\mu_0 S_a}, \tag{5}$$

$$S_m = S_a = S, \tag{6}$$

where l_m is the length of the path along the magnetic material, $\mu = 4\pi \cdot 10^{-7}$ H $\cdot$ m^{-1} is the magnetic permeability of air, μ_r is the permeability of magnetic material and l_a is the length of the air gap. By combining the equations in expression (Eq. (2)) and expression (Eq. (5)), the magnetic induction equation is obtained:

$$\frac{\Phi}{\mu S}\left(\frac{l_m}{\mu_r} + l_a\right) = NI \rightarrow \Phi = \frac{\mu_0 S \cdot NI}{\left(\frac{l_m}{\mu_r} + l_a\right)} = BS, \tag{7}$$

$$B = \frac{\mu_0 NI}{\left(\frac{l_m}{\mu_r} + l_a\right)}. \tag{8}$$

From the definition of Maxwell Stress Tensor and the properties of Kronecker delta, considering the fact that the magnetic field B has only y component (Fig. 2), it is possible to write the electromagnetic force acting on the plunger of EMA as [13]:

$$\sigma_{xx} = \frac{1}{\mu_0} B_x B_x - \frac{1}{2\mu_0} B^2 \delta_{xx}, \tag{9}$$

$$\sigma_{xx} = \frac{1}{\mu_0} B^2 - \frac{1}{2\mu_0} B^2 = \frac{B^2}{2\mu_0} = F. \tag{10}$$

By combining the Eq. (8) and Eq. (10), the final equation for electromagnetic force (F_e) acting on the plunger is obtained:

$$F_e = \frac{\mu_0 \left(NI\right)^2 S}{2\left(\frac{l_m}{\mu_r} + l_a\right)^2}. \tag{11}$$

The cross-section area of the plunger can be obtained using the equation:

$$S = \pi \cdot \left(r_{po}^2 - r_{nms}^2\right), \tag{12}$$

where r_{po} is the plunger outer radius and r_{nms} is the radius of non-magnetic shaft. Length of the path along the ferromagnetic material (Fig. 2) is calculated using the following equation:

$$\begin{aligned} l_m &= 2l_x + 2l_y - l_a = \\ &= 4t_{co} + 2w_c + 2h_c - l_a, \end{aligned} \tag{13}$$

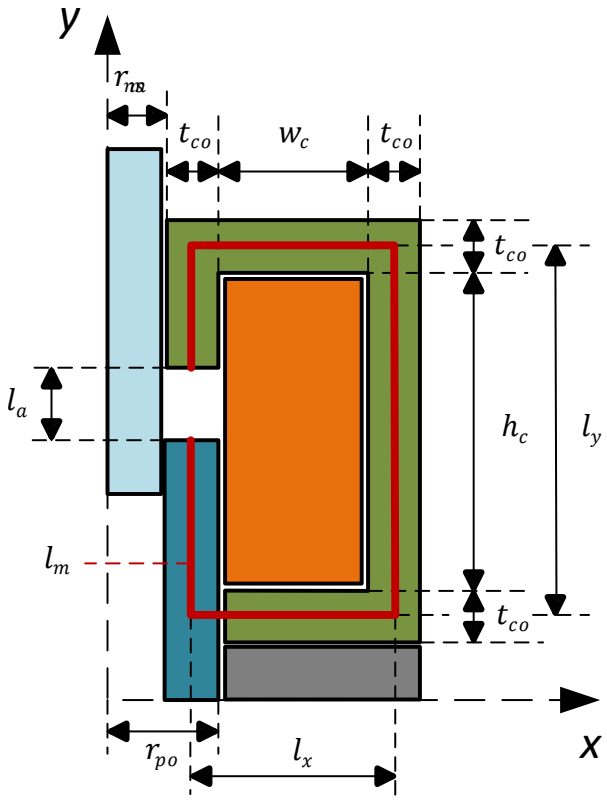

Fig. 2: Design variables overview.

with the following notations: l_x, l_y - the paths along the magnetic material in the x and y direction, t_{co} - the thickness of core, w_c - the coil width and h_c - the coil height.

To calculate the coil height, the Pappus centroid theorem for volume of solids of revolution is used:

$$V = 2\pi \cdot A \cdot d = L \cdot A_w = \frac{R}{R_{lin}} \cdot A_w, \tag{14}$$

where A is the area of the surface which is rotating, d is the distance of its geometric centroid from the axis of revolution, L is the length of wire, A_w is the area of the wire cross section, R is the coil resistance and R_{lin} is the linear resistance. The distance and area can be obtained using the equations:

$$d = r_{po} + \frac{w_c}{2}, \tag{15}$$

$$A = N_x \cdot N_y \cdot A_w, \tag{16}$$

$$N_y = \frac{h_c}{D_w}. \tag{17}$$

By combining the Eq. (14), Eq. (15), Eq. (16) and Eq. (17) the equation for calculation of the coil height is obtained:

$$h_c = \frac{D_w \cdot L}{\pi \cdot N_x \cdot (2r_{po} + w_c)}. \tag{18}$$

The coil width is dependent on the coil turn arrangement. The angle between wires affects the coil width (Fig. 3).

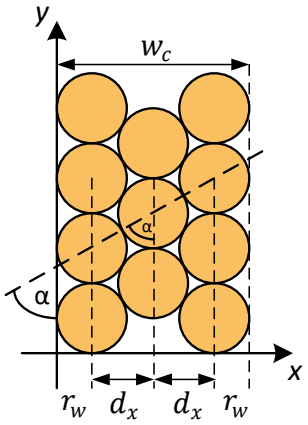

Fig. 3: The coil turn arrangement.

In order to obtain the dependence of winding angle to the coil width, the following relations can be written from Fig. 3 [14]:

$$N_x = 3, \tag{19}$$

$$d_x = 2r_w \sin\alpha = D_w \sin\alpha, \tag{20}$$

$$w_c = 2r_w + 2d_x = D_w + (N_x - 1)\, D_w \sin\alpha, \tag{21}$$

$$w_c = D_w \left[1 + (N_x - 1)\sin\alpha\right], \tag{22}$$

with following notation: r_w - the wire radius, α - the angle between windings and d_x - the distance between two windings in x direction. The total number of turns (N) is defined as:

$$N = N_x \cdot N_y = N_x \cdot \frac{hc}{D_w} = \frac{L}{\pi\left(2r_{po} + w_c\right)}. \tag{23}$$

The length of wire has been already defined in Eq. (14), but it can be also written as:

$$L = \frac{R_0}{R_{lin}} = \frac{U}{R_{lin} \cdot I} = \frac{4U}{R_{lin} \cdot J_{\max} \pi D_{iw}^2}, \tag{24}$$

where $J_{\max}$ is the maximum current density and D_{iw} is the inner wire diameter. Substituting Eq. (23) and Eq. (24) into Eq. (11) results in the final equation for electromagnetic force:

$$F_e = \frac{\mu_0 U^2 \left(r_{po}^2 - r_{nms}^2\right)}{2R_{lin}^2 \pi \left(2r_{po} + D_w\left[1 + (N_x - 1)\sin\alpha\right]\right)^2} \cdot \frac{1}{\left(\frac{(4t_{co} + 2D_w[1 + (N_x - 1)\sin\alpha] + 2h_c - l_a)}{\mu_r} + l_a\right)^2}. \tag{25}$$

From the equation Eq. (25), it can be clearly seen the electromagnetic force dependence on the angle between windings.

4. Coil Winding Angle Impact - Numerical Analysis

Dynamic modeling of EMA's time response is difficult because of the need to simultaneously solve non-linear differential equations of its magnetic, electrical and mechanical subsystem [15]. The equations which lead to time and space dependent electromagnetic magnitudes and which are also used to solve the magnetic subsystem of EMA are well known Maxwell's equations. In the case of axial-symmetric geometry, the vector potential A has only one component and that scalar function depends on two space variables (r, z) and time (t) [16]. The final expression for time dependable differential equation of magnetic subsystem is [17]:

$$\frac{\partial}{\partial r}\left(\frac{1}{\mu \cdot r} \cdot \frac{\partial}{\partial r} \cdot (r \cdot A_\varphi)\right) + \frac{\partial}{\partial_z}\left(\frac{1}{\mu} \cdot \frac{\partial A_\varphi}{\partial z}\right) = = \frac{N \cdot i}{S_c} - \sigma \frac{\partial A_\varphi}{\partial z} \sigma \cdot v \frac{\delta A_\varphi}{\delta z}, \tag{26}$$

where A_φ is the circular component of the magnetic vector potential, S_c is the cross-section area of coil, σ is the electric conductivity and v is the plunger velocity. The voltage equilibrium equation in the circuit is defined as:

$$u = R \cdot i + \frac{2\pi \cdot N}{S_c} \int_{S_c} \frac{\partial}{\partial t} (r \cdot A_\varphi)\, \mathrm{d}S_c, \tag{27}$$

where u is the voltage supply and R is the coil resistance. The position of the movable plunger is defined by the following equation of motion:

$$m\frac{\mathrm{d}v}{\mathrm{d}t} + \beta \cdot v = F_e - F_l, \tag{28}$$

where m is the plunger mass, β is the damping coefficient, v is the velocity of plunger movement in z direction and F_l is the load force. The plunger velocity in z direction is given as:

$$v = \frac{\mathrm{d}z}{\mathrm{d}t}. \tag{29}$$

The calculation of electromagnetic force acting on the plunger, in every time step, is performed from the magnetic energy change:

$$F_e = \frac{\mathrm{d}W}{\mathrm{d}z} = \frac{\partial}{\partial z}\left[\int_V \left(\int_0^H B dH\right) \mathrm{d}V\right], \tag{30}$$

where W is the magnetic energy, H is the magnetic field strength and V is the volume of EMA. The magnetization curve of used magnetic material is illustrated in Fig. 4. The electromagnetic calculation is performed using ANSYS Electronics software package.

The numerical simulation is performed on the two models of solenoid EMA (Fig. 5). Both have the same

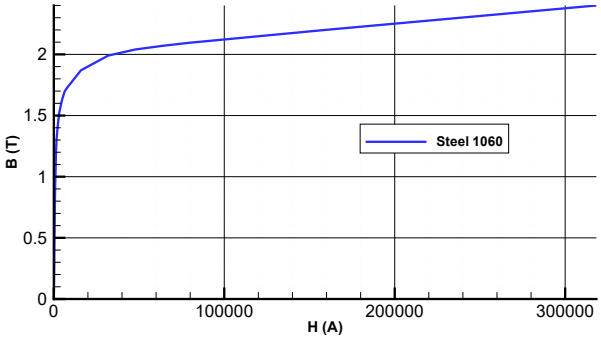

Fig. 4: *B-H* curve of used magnetic material.

excitation voltage (U), coil resistance (R), coil height (h_c) and plunger dimensions, but different coil width (w_c) and angle between coil turns (α). The model in Fig. 5(a) is simulated for 90 degrees ($\alpha = 90°$) angle between coil turns, while the model in Fig. 5(b) is simulated for 60 degrees angle ($\alpha = 60°$). Dirichlet's boundary condition for magnetic field (($A_\varphi = 0°$)) has been applied to the outer edge of the models. This results in magnetic flux to be tangential to the model boundary, confining the flux within the model. The coils were modeled according to the calculated number of turns in x direction. The fixed design variables of simulated EMA are given in Tab. 2.

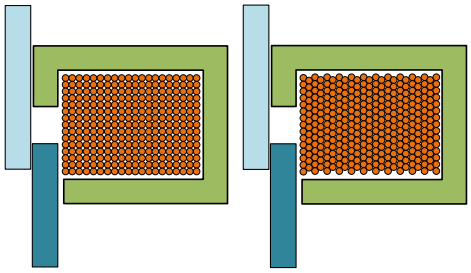

(a) $\alpha = 90°$. (b) $\alpha = 60°$.

Fig. 5: 2D axial-symmetric model of solenoid EMA.

Tab. 2: Values of fixed design variables.

	Label	Description	Value
1.	r_{nms}	Non-magnetic shaft radius	1 mm
2.	r_{po}	Plunger outer radius	3 mm
3.	t_{co}	Core thickness	2 mm
4.	h_c	Coil height	4.92 mm
5.	l_a	Air gap length	2.5 mm
6.	N_y	Number of turns in y direction	20
7.	D_w	Wire diameter	0.24 mm
8.	D_{iw}	Inner wire diameter	0.2 mm

The simulation time step is set to 0.05 ms, while the total duration of the simulation is set to 5 ms. The load force (F_l) consists of a constant component, preload spring force (F_1), on which the variable spring force modeled as function of plunger displacement is superposed:

$$F_l = F_1 + ky, \tag{31}$$

where k is the spring constant and y is the plunger displacement. Numerical simulation results of the plunger displacement and electromagnetic force acting on the plunger are shown in Fig. 6.

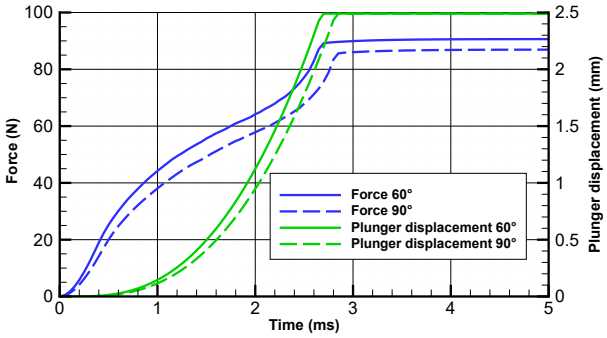

Fig. 6: Comparison of numerical simulation results.

Figure 6 shows that electromagnetic force produced by coil turns at angle of 60 degrees achieves higher values of force from the beginning of the simulation. Also, it can be seen that coil winding angle has an impact on the time response of EMA, which has not been included in analytical analysis. The time response is improved for 5.26 % by winding the coil at an angle of 60 degrees. At maximum plunger displacement, the dynamic electromagnetic force has its maximum value in amount of 86.91 N for the model with an angle of 90 degrees between the coil turns, while the maximum force for the model with an angle between the coil turns of 60 degrees is 90.62 N. By using the coil, which has the angle of 60 degrees between the coil turns, the maximum value of electromagnetic force is increased for 4.27 %.

5. Comparison of Numerical and Analytical Results

In order to compare analytical and numerical simulation results, the numerical magnetostatic calculation have been done. Both, the analytical and numerical results show that the amount of force acting on the plunger of solenoid EMA is bigger if the coil winding angle is smaller. The results are shown in Tab. 3.

The analytical calculation does not consider the nonlinear *B-H* curve of the material. It neglects the fringing flux effect in the air gap, the impact of the small air gaps and the impact of the coil insulation. It gives the approximate results of the electromagnetic force amount which in the worst case have the maximum deviation of 17 % compared to the results of numerical simulations (Fig. 7).

Tab. 3: Comparison of analytical and numerical results.

Plunger Displacement (mm)	Force (N) - 90° (Analytical)	Force (N) - 60° (Analytical)	Force (N) - 90° (Numerical)	Force (N) - 60° (Numerical)
0	29.02	37.30	28.59	32.30
0.5	33.79	43.71	33.73	37.44
1.0	39.83	51.93	39.67	43.38
1.5	47.64	62.70	47.48	51.19
2	58.00	77.21	60.98	64.69
2.5	72.13	97.4	86.91	90.62

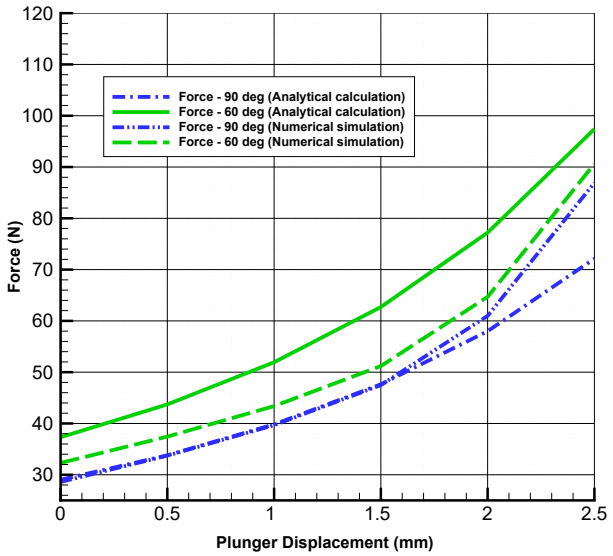

Fig. 7: Comparison of numerical and analytical results.

6. Conclusion

The aim of any EMA development is to develop an actuator with higher electromagnetic force acting on the plunger, with as fast time response as possible, while maintaining the dimensions as small as possible.

In this paper, the impact of coil winding angle on the force of DC solenoid EMA is observed, where the coil resistance and coil height are fixed, while coil width depends on the coil winding angle. The coil winding angle directly determines coil filling factor, which is the largest at the ideal winding angle of 60 degrees and its value in that case is 0.907.

The results of numerical simulations have shown that, by reducing the coil winding angle, it is possible to increase the electromagnetic force by 4.27 %. Also, by reducing coil winding angle, compared to the worst angle (90°), it is possible to reduce the coil dimensions, and thus the dimensions of electromagnetic actuator. The results of numerical simulations were compared to the results of analytical calculations and a maximum deviation of 17 % was established. In order to reduce this percentage, an analytical model needs to be upgraded in further work.

References

[1] PLAVEC, E. and M. VIDOVIC. Genetic algorithm based plunger shape optimization of DC solenoid electromagnetic actuator. In: *2016 24th Telecommunications Forum (TELFOR)*. Belgrade: IEEE, 2016, pp. 1–4. ISBN 978-1-5090-4086-5. DOI: 10.1109/TELFOR.2016.7818839.

[2] MAYER, D. and B. ULRYCH. Analysis of an electromagnetic actuator with permanent magnet. *Advances in Electrical and Electronic Engineering*. 2006, vol. 5, no. 1, pp. 301–305. ISSN 1804-3119.

[3] CVETKOVIC, D., I. COSIC and A. SUBIC. Improved performance of the electromagnetic fuel injector solenoid actuator using a modelling approach. *International Journal of Applied Electromagnetics and Mechanics*. 2008, vol. 27, iss. 1, pp. 251–273. ISSN 1875-8800.

[4] PLAVEC, E., I. UGLESIC and M. VIDOVIC. Genetic Algorithm Based Shape Optimization Method of DC Solenoid Electromagnetic Actuator. *Applied Computational Electromagnetics Society Journal*. 2018, vol. 33, no. 3, pp. 325–335. ISSN 1054-4887.

[5] GOSIEWSKI, Z. and M. KONDRATIUK. Selection of Coils Parameters in Magnetic Launchers. *Solid State Phenomena*. 2009, vol. 147, iss. 1, pp. 438–443. ISSN 1662-9779. DOI: 10.4028/www.scientific.net/SSP.147-149.438.

[6] MARDER, B. A coilgun design primer. *IEEE Transactions on Magnetics*. 1993, vol. 29, iss. 1, pp. 701–705. ISSN 1941-0069. DOI: 10.1109/20.195661.

[7] MENG, F., G. TAO and P. P. LUO. Dynamic analysis of proportional solenoid for automatic transmission applications. In: *2014 International Conference on Mechatronics and Control (ICMC)*. Jinzhou: IEEE, 2014, pp. 1120–1124. ISBN 978-1-4799-2538-4. DOI: 10.1109/ICMC.2014.7231727.

[8] PETRARCA, C., G. LUPO, V. TUCCI and M. VITELLI. The influence of coil parameters on

the voltage distribution in a machine stator winding fed by a PWM inverter. In: *2000 Annual Report Conference on Electrical Insulation and Dielectric Phenomena (Cat. No. 00CH37132)*. Victoria: IEEE, 2000, pp. 490–493. ISBN 0-7803-6413-9. DOI: 10.1109/CEIDP.2000.884005.

[9] LATIF, N. A. A., I. M. Z. ABIDIN, M. DOLLAH and A. N. IBRAHIM. A study on effects on size and coil's turns based on signal distribution on impedance plane diagram. *Journal of Industrial Technology*. 2006, vol. 26, no. 4, pp. 1–7.

[10] ZHANG, L., K. YANG, Z. LIU, Y. GENG and J. WANG. Influence of design parameters on electro-magnetic repulsion mechanism performance. In: *2016 27th International Symposium on Discharges and Electrical Insulation in Vacuum (ISDEIV)*. Suzhou: IEEE, 2016, pp. 1–4. ISBN 978-1-4673-9780-3. DOI: 10.1109/DEIV.2016.7763973.

[11] NARAYANSWAMY, R., D. P. MAHAJAN and S. BAVISETTI. Unified coil solenoid actuator for aerospace application. In: *2012 Electrical Systems for Aircraft, Railway and Ship Propulsion*. Bologna: IEEE, 2012, pp. 1–5. ISBN 978-1-4673-1372-8. DOI: 10.1109/ESARS.2012.6387392.

[12] JILES, D. *Introduction to magnetism and magnetic materials*. 3rd ed. Boca Raton: CRC Press, 2016. ISBN 978-1-4822-3888-4.

[13] LABBE, T. and B. DEHEZ. Topology Optimization Method Based on the Maxwell Stress Tensor for the Design of Ferromagnetic Parts in Electromagnetic Actuators. *IEEE Transactions on Magnetics*. 2011, vol. 47, iss. 9, pp. 2188–2193. ISSN 1941-0069. DOI: 10.1109/TMAG.2011.2138151.

[14] RIGHETTI, D. *Solenoid Actuators*. 1st ed. Tricase: Youcanprint SelfPublishing, 2017. ISBN 978-8-8926-7112-6.

[15] BRAUER, J. R. *Magnetic Actuators and Sensors*. 2nd ed. Hoboken: Wiley-IEEE Press, 2014. ISBN 978-1-118-50525-0.

[16] MAHAJAN, D. P., R. NARAYANASWAMY and S. BAVIASETTI. Performance analysis and experimental verification of solenoid actuator. In: *2014 IEEE 23rd International Symposium on Industrial Electronics (ISIE)*. Istanbul: IEEE, 2014, pp. 1245–1249. ISBN 978-1-4799-2399-1. DOI: 10.1109/ISIE.2014.6864792.

[17] ANSYS Electronics Desktop Script. In: *ANSYS* [online]. 2018. Available at: `www.ansys.com`.

About Authors

Eduard PLAVEC was born in 1988 in Zagreb, Croatia. He received the Ph.D. degree in 2018. at University of Zagreb, Faculty of Electrical Engineering and Computing where he also received his B.Sc. and M.Sc. degrees in Electrical Engineering and Information Technology in 2011. and 2013., respectively. He joined KONCAR Electrical Engineering Institute in 2014., where he began as a research and development engineer in the field of electromagnetics at Switchgear and Controlgear Department. His areas of interest include computational electromagnetics and high-voltage engineering. He is a member of the CIGRÉ Study Comitee A3 - High voltage equipment, IEEE member since 2012 and ACES member from 2016.

Ivan LADISIC was born in 1981 in Zagreb, Croatia. He received M.Sc. degrees in Electrical Engineering and Information Technology in 2007. at University of Zagreb, Faculty of Electrical Engineering and Computing. He works in KONCAR Electrical Engineering Institute as a researcher since 2007 at Switchgear and Controlgear Department. His area of interest are development of high voltage switchgears, computational electromagnetics and high-voltage engineering.

Mladen VIDOVIC was born in Zagreb, Croatia. He received his B.Eng. degree from University of Zagreb, Faculty of Electrical Engineering in 1984. He has been working in KONCAR Electrical Engineering Institute since 1986, at Switchgear and Controlgear Department where he is currently the Head of Research and Development Section. His areas of interest are design and diagnostic of high-voltage switchgears and development of on-line monitoring systems of high-voltage apparatus. He is the author of several papers and patents.